RETENTION AND FEATURES OF DEUTERIUM DETRAPPING FROM RADIATION-INDUCED DAMAGES IN STEELS

G.D. Tolstolutskaya, V.V. Ruzhytskiy, S.A. Karpov, I.E. Kopanets

National Science Center "Kharkov Institute of Physics and Technology", Kharkov, Ukraine

E-mail: g.d.t@kipt.kharkov.ua

The accelerators and ion-beam analysis techniques are used for simulation of displacement damage and detailed investigation of distribution profiles of damage and impurity gas atoms (especially helium and hydrogen) in the irradiation of targets for a wide ranges of doses and particle energies. The influence of preimplanted helium and heavy ion-induced damage on deuterium trapping in austenitic and ferritic/martensitic steels was studied. The results obtained for 18Cr10NiTi stainless steel show that ion-implanted deuterium is weakly trapped by defects produced in 5 keV D^+ displacement cascades. The effective trapping temperature interval is between 300 and 600 K. The characteristics of trapping and the temperature range of hydrogen isotopes retention in traps formed by prior implantation of helium depend on the concentration of implanted helium and on the type of defects developed. The formation of helium bubbles in 18Cr10NiTi steel causes an order of magnitude increase in the content of retained deuterium atoms in the range of temperature 300-600 K and extends the interval of effective trapping temperatures to 1000 K. Energetic heavy-ion irradiation (1.4 MeV Ar^+) has been used for modeling defect cluster formation under displacement cascade conditions to simulate fusion reactor environments. It was found that retention of hydrogen and deuterium strongly increased in this case. It is shown that the presence of a surface-passive film considerably shifts the gas release interval to higher temperatures and reduces the deuterium surface recombination coefficient by several orders of magnitude.

I. INTRODUCTION

Recent investigations on radiation damage phenomena have been making remarkable progress. Still there is a long way to gain clear understanding of the material behavior in fission and fusion environments. In this situation, charged particle-material interaction studies using accelerators may contribute to advanced materials R & D.

The interactions of hydrogen and helium with defects in solids play an important role in the mechanical behavior of various materials. Hydrogen and helium atoms are generated by nuclear transmutation in fusion and fission reactors, spallation neutron sources and high energy charged particle environments. Garner and coworkers have recently shown that in fission reactors rather high concentrations of hydrogen can accumulate in stainless steels [1]. It appears that hydrogen gas can be stored in irradiated metals at concentrations significantly in excess of that predicted by Sieverts' law, providing that cavities such as bubbles or voids are formed. The current hypothesis is that hydrogen is stored as H_2 gas in such cavities. In order to explain such storage it is required that supersaturations of atomic hydrogen be maintained in metals by various transmutation, radiolytic or environmental sources [2].

The retention and accumulation of hydrogen in irradiated materials are most likely caused by the presence of high concentrations of microstructural trapping sites. It was assumed that helium bubbles and voids were the operating traps [3]. On the other hand, the elastic fields around defect clusters are considered by some researchers as the trap for retaining hydrogen [4]. Further experiments are necessary to solve some of these problems.

In a fusion reactor, the synergistic effect of displacement damage, helium and hydrogen atoms can enhance the irradiation-induced degradation. Such effects were observed in a number of investigations. The highest swelling has been observed in ferritic model alloys of Fe-Cr under triple ion irradiation [5]. In vanadium alloys, simultaneous irradiation of Ni, He and H ions enhanced cavity formation and swelling [6]. The synergistic effect of He

and H irradiation in these alloys and F82H martensitic steel [7] was confirmed by the occurrence of larger cavities and higher swelling under triple ion irradiation as compared with dual ion irradiations.

In the present work, the measuring system "ESU-2" and accelerator "Ant" have been used to study deuterium retention and effects of the interaction between deuterium, noble gases and defects in austenitic and ferritic/martensitic steels. We have used a beam of argon ions to simulate the displacement damages produced by high energy neutrons.

II. THE EQUIPMENT AND EXPERIMENTAL PROCEDURE

The measuring system consists of a compact electrostatic accelerator "ESU-2 MeV", a mass-separator, an implanter, chambers for target irradiation and measurements using the methods of Rutherford backscattering, channeling and nuclear reactions. The accelerating installation "Ant" is intended for irradiation of specimens by beams of gaseous ions and investigated of deuterium desorption behavior. The conditions of materials irradiation are summarized in Tabl. 1.

Table 1

Irradiation conditions

Equipments	Ion	Energy, keV	Ion flux, $cm^{-2} \cdot s^{-1}$	Energy stability, %
The measuring system "ESU-2"	Inert gas from **He** to **Xe,** chemically active from **hydrogen** to **nitrogen**	**200-1600** (3200 for double-charged ions)	**10^{13}….10^{14}**	**0.1**
Accelerator "ANT"	**H, H_2, D, D_2, He, N**	**20-100 (I) 15 (II)**	**10^{12}….10^{14}**	**0.5**

II.A. Facility for triple-ion irradiation

The ions of argon and krypton were chosen because irradiation with these ions with energies between 1 and 3.2 MeV can cause damage production at the level of 100 to 200 dpa at a depth of 500 nm from the surface. The time to achieve 100-200 dpa was ~2-4 hour at the area of irradiation ~0.1 cm^2.

Computations with the program SRIM 2003 [8] have shown that for introduction of helium and hydrogen (deuterium) in the region of damage, it is necessary that particles should have an energy of about 50 keV (helium) and 25 keV (hydrogen/deuterium) (Fig.1). For the solution of different tasks it is desirable to provide the possibility of varying particle energies in the 3 to 50 keV range.

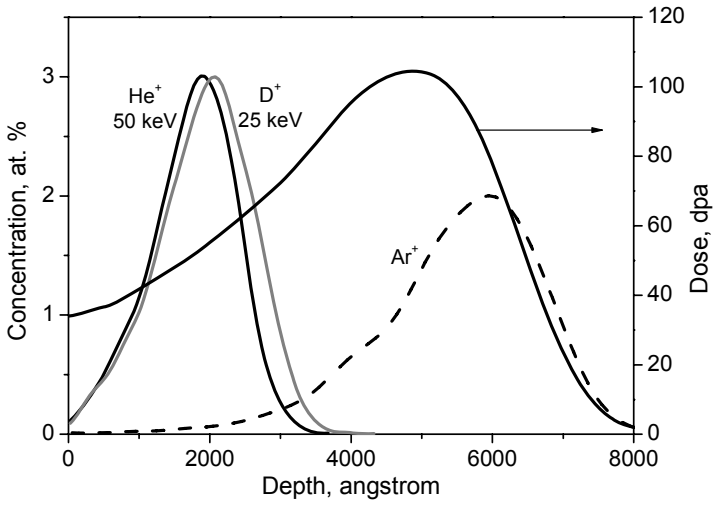

Fig. 1. Calculated distribution profiles of helium, deuterium and argon ions of energies 50, 25 and 1400 keV in stainless steel, respectively

Simultaneous implantation of helium and hydrogen may be performed by means of two irradiation facilities (Fig. 2) that include:

- ♦ Ion injector with a gas inlet system;
- ♦ Accelerating system;
- ♦ Base chamber;
- ♦ Magnetic mass-analyzer;
- ♦ Vacuum-pumping system;
- ♦ High-voltage power supply 0-50 kV;
- ♦ Electrical power supply for the ion injector.

The difference is only in the gas introduced into the injector: in one facility it is helium, in the other − deuterium or hydrogen.

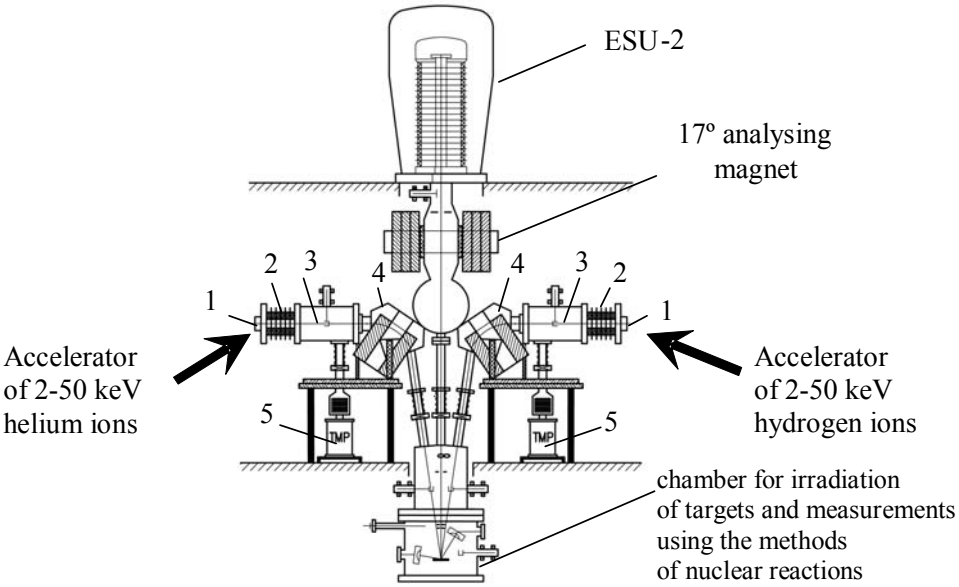

Fig. 2. Diagram of measuring complex ESU-2: 1 − ion injector; 2 − accelerating system; 3 − base chamber; 4 – electromagnet; 5 − turbomolecular pump

The assembly has an oil-free pumping system with a residual target-chamber pressure of $\sim 1 \cdot 10^{-4}$ Pa. The helium ion flux was 10^{13} $cm^{-2} \cdot s^{-1}$, and the deuterium ion flux was 10^{14} $cm^{-2} \cdot s^{-1}$. The implantation temperature ranged from 300 to 900 K. Post-implantation annealing of specimens was performed in the temperature range 300-1200 K by ohmic heating at the rate of 7 $K \cdot s^{-1}$.

The measuring system "ESU-2" allows the use of various ion beam analysis techniques, including Rutherford backscattering spectroscopy (RBS), channeling, nuclear reaction analysis (NRA) (Tabl. 2). The ion beam technique and methodologies for the analysis of experimental data provide a comprehensive tool for studying crystal defects.

Table 2

Some characteristics of analytical techniques which using on the "ESU-2" facility

Analytical techniques	Detection of Elements, Z	Depth Resolution, Å	Analyzing Layers, μm	Limit of Detection, mass.%
NRA	≥1	50-300	1-10	$10\text{-}10^{-5}$
RBS	≥2	100	1-3	$10^{-1}\text{-}10^{-6}$
Channeling	≥2	100	1-3	$10^{-1}\text{-}10^{-6}$

The substitution of deuterium for protium allows the use of nuclear reaction profiling to determine the depth distribution and the concentration of hydrogen isotopes. Irradiations and measurements by nuclear methods were performed in one chamber, excluding contact of the specimens with air that prevented the formation of artifact trap sites associated with the surface oxide [9]. The implanted particle depth distribution was measured using the nuclear reactions $^3He(D,p)^4He$ and $D(^3He,p)^4He$. The measurements were performed using forward and back scattering geometries.

In the forward geometry, 700-keV ^3He or 1000-keV D_2 was used to analyze the near-surface region that contained deuterium or helium. With a solid-state detector and

standard electronics, the energy spectrum of α-particles (emitted in the nuclear reaction at different depths at a rate proportional to the local deuterium concentration) was obtained and the deuterium or helium depth profile was deduced. The beam of either ^{3}He or deuterium ions was incident at an angle of 30^o to the specimen surface and the nuclear reaction products were detected at an angle of 60^0 with respect to the analyzing beam. The beam diameter was 4 and 2 mm during irradiation and analyzing runs, respectively. The depth resolution in the forward scattering geometry was determined to be ~20 nm. The probing depth was approximately 0 to 0.3 μm. To determine the true depth profile, the experimental spectrum was fitted by using the GANRA program [10], in which cross-section of reaction D(^{3}He,p)^{4}He was taken from [11], range and straggling of ions ^{3}He and ^{4}He was calculated according to Ziegler, angle distribution of ^{3}He in given layer of target was computed by program SRIM [8].

In the backscattering geometry, the protons from D (^{3}He,p)^{4}He or ^{3}He(D,p)^{4}He reactions were measured by the surface-barrier detector tilted at 157^o to the incident beam. The energy spectra of protons Y(E) were measured in the 0.3-1.6 MeV energy range. For the backscattering geometry the probing depth was 0 to 1.8 μm.

II.B. Facility for double-ion irradiation

The multipurpose compact accelerating installation "Ant" is intended for irradiation of specimens by beams of gaseous ions with different energy spectra (E~2-100 keV) (Fig. 3). The selected energy range of the two beams allows us to interrelate space-concentration distributions of helium and hydrogen on the one hand, and to investigate the behavior of He and H at different combinations of distributions on the other hand.

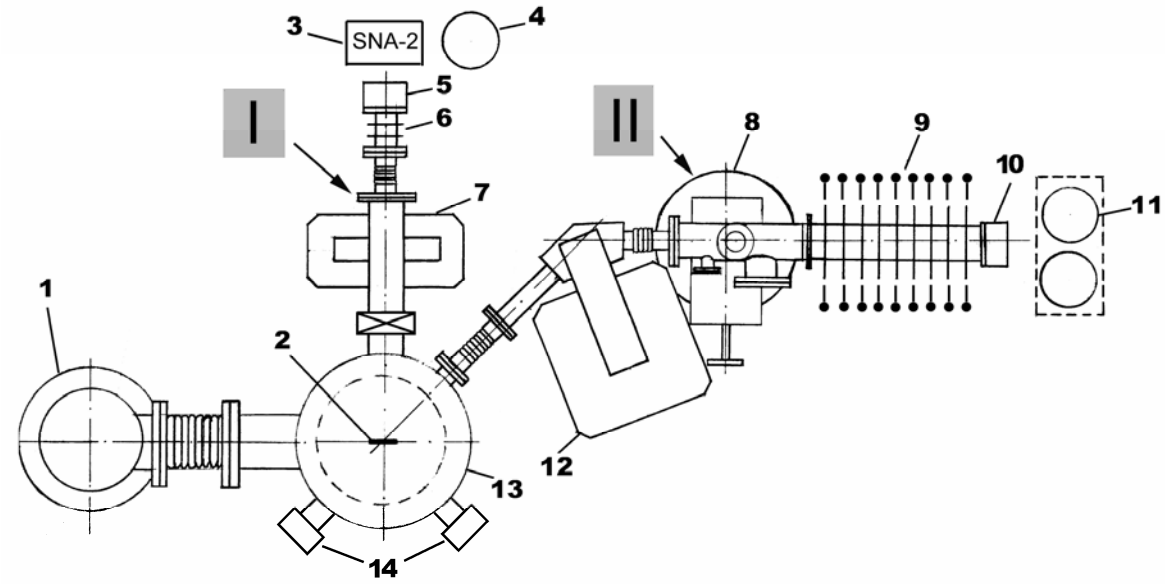

Fig.3. Diagram of accelerating facility "Ant":
1 and 8 – turbomolecular pump; 2 – specimen; 3 – gas inflow system; 4 and 11 – system of electric power supply; 5 and 10 – ion source; 6 – three-electrode electrostatic lens; 7 and 12 – magnetic mass-separator; 9 – accelerating tube; 13 – target chamber; 14 – mass-spectrometer measuring elements

The assembly consists of three different parts: two ion-accelerating sections I and II and the target chamber with two mass-spectrometers.

Accelerating section I includes an ion source (5) (Penning source-type), three-electrode electrostatic lens (6), and a mass-separator of ions (7). The ion source can provide beams of H^+, H_2^+, D^+, D_2^+, He^+, N^+ ions for injecting them into the accelerating system. The gas is let into the ion source with the aid of the electro mechanical system SNA-2. The electromagnetic mass-separator of ions (7) provides the ion beam rotation through 15^o.

Accelerating section II comprises an ion source (10) (Penning source-type), 9-section accelerating tube (9), and an ion mass-monochromator (12). The electromagnetic mass-separator of ions (12) deflects the ion beam through 45°. The accelerating section is degassed by a high-vacuum pumping system (8) that guarantees the background pressure to less than $1 \cdot 10^{-5}$ Pa. The two detectors of the two monopole mass-spectrometers (14) are connected to the target chamber to measure the partial pressure of gases. The vacuum pumping system for the target chamber is a turbomolecular pump with a nitrogen trap (1). The accelerating section I provides ion beams of energies up to 15 keV, and section II provides ion beams in the range 20-100 keV.

The present paper discusses the application of the above facilities for an integrated study of the displacement damage and detailed depth profiling of damage and impurity atoms in the irradiation of structural steels over a wide range of doses of heavy particles, helium and deuterium.

III. EXPERIMENTAL DETAIL

The specimens used were foils of austenitic 18Cr10NiTi and ferritic EI852 steels. The 18Cr10NiTi steel is used in the states of the former Soviet Union for nuclear applications, where AISI 304 would be used in Western countries. Its composition is similar to AISI 321 (Fe-18.5Cr-9.5Ni-1.5Mn-0.7Si-0.6Ti with ≤0.08C). Specimen dimensions were 27x7x0.1 mm which were cut from 18Cr10NiTi steel, following annealing for 1 hour at 1340 K in 10^{-4} Pa vacuum. The specimens were polished in electrolyte of composition 54% H_3PO_4, 11% H_2SO_4, 21% H_2O, and 14% CrO_3. Prior to irradiation, the specimens were short-term annealed to 1200 K in the experimental chamber for surface cleaning and degassing.

The specimens were irradiated with 1400 keV Ar^+ at room temperature up to doses of $1 \cdot 10^{20}$ to $1 \cdot 10^{21}$ Ar/m^2. A beam of argon ions was incident at angles of 90 and 30° with respect to the surface. These angles were chosen to provide the deuterium location in the damage region only (90°) or in the region of damage and required argon atoms concentration (30°). The implantation temperature was 300 K and was monitored using a chromel-alumel thermocouple. The SRIM code [8] was used to evaluate the ion projected ranges (R_p) and range straggling (ΔR_p), as well as the energies deposited in nuclear collisions (E_v), the concentration of gas atoms (C) and the number of displacements per atom (dpa), all created at depths 0-100 nm. The calculations were performed with a target density of 7.9 g·cm^{-3} and displacement threshold energies of 40 eV. Deuterium release from stainless steel samples was investigated using the thermodesorption mass-spectrometry technique. The microstructure of the implanted 18Cr10NiTi steel was examined by means of transmission electron microscopy at room temperature, employing standard bright–field techniques on the EM-125 electron microscope.

Results and discussion

The amount of deuterium retained in the specimens at T_{room} was ~80% relative to the irradiation dose (for spectrum measured for ~15 min after irradiation termination and dose interval 10^{19}-10^{20} D/m^2). The nuclear reaction profiling and the thermal desorption measurements have shown that the effective temperature interval for trapping deuterium implanted in SS to a fluence of $1 \cdot 10^{20}$ D/m^{-2} lies between 300 and 600 K (Fig. 4). The desorption is characterized by two stages of gas release.

In order to deduce the deuterium trapping parameters we have modeled the implantation, diffusion, trapping, detrapping, and recombination processes that occur during the experiment. In the model, deuterium is implanted in the sample at a distance *(x)* from the surface having the profile *G(x)* obtained from nuclear reaction profiling measurements [10] for 5 keV D^+. The modeling calculation is a numerical solution for the diffusion of deuterium in the presence of trapping sites and has been discussed in detail elsewhere [12]. By comparison of experimental curves with calculation data it has been established that ion-implanted deuterium is trapped by radiation defects with binding energies of 0.28 and 0.36 eV (see Fig. 4). It was suggested that D atoms were trapped in vacancies and at higher doses – in vacancy clusters [12].

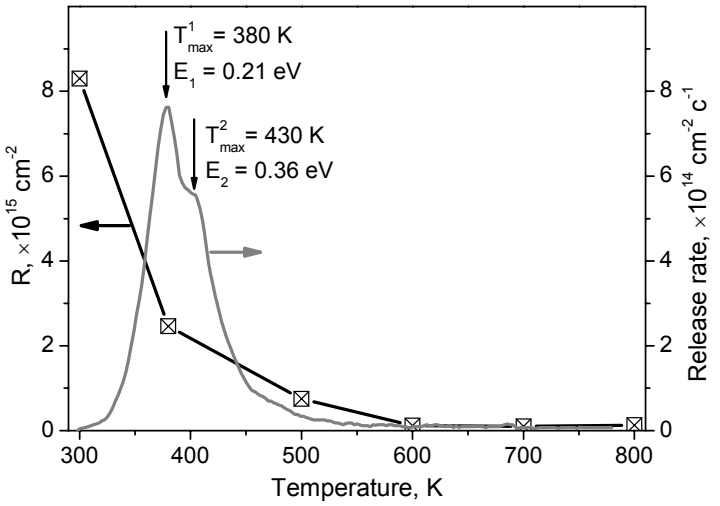

Fig. 4. Linear temperature ramp thermal desorptions (grey curve) and temperature-dependent areal densities (R) (black curve) of deuterium implanted into 18Cr10NiTi SS

Fig. 5 shows the exposure time dependence of deuterium retention in steel at RT after irradiation with fluence of $1 \cdot 10^{20}$ D/m^2. The data presented in Aig. 5 were obtained by using the NRA and TDS experimental techniques. The deuterium retention is decreasing throughout the time interval under study, especially drastically during the first several hours.

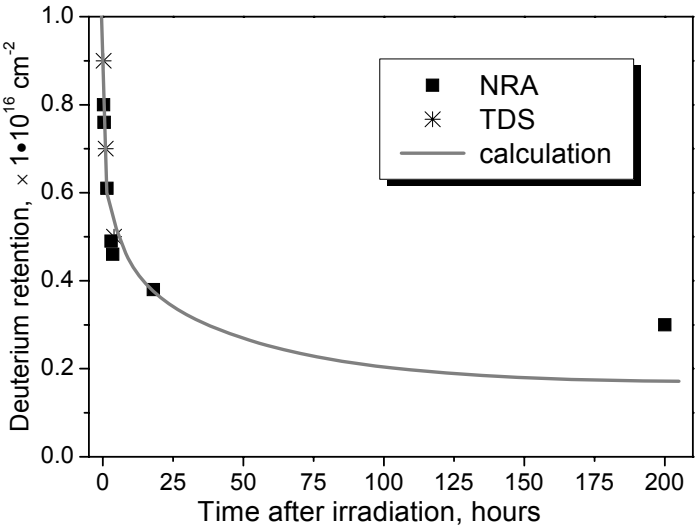

Fig.5. Deuterium retention as a function of time for stainless steel samples implanted with 5 keV D ions to a fluence of $1 \cdot 10^{20} m^{-2}$

The calculations of deuterium retention during isothermal annealing of specimens at T=300 K (Fig.5) were performed with thermodynamic parameters obtained by fitting the experimental curve shown in Fig. 4. The modeling calculation gives a good description of the data for the exposure time of ~25 hours. The differences that are observed between the experiment and the calculated deuterium retention curves at large exposure times are related to the blocking influence of the growing superficial oxide layer. The data presented in Figs. 4 and 5 show that the ion-implanted deuterium is weakly trapped by defects produced in low-energy displacement cascades. There have been numerous investigations into the behaviour of hydrogen in austenitic stainless steel. Three phenomena

have been characterized: 1) trapping by He bubbles, 2) trapping of hydrogen by irradiation defects, and 3) surface-controlled release from solution to the gas phase.

Trapping by He bubbles. Recently [13], it has been shown that helium pre-implantation into 18Cr10NiTi steel causes the formation of traps that can retain hydrogen isotopes in a wider range of temperatures, 500-1000 K in comparison with deuterium irradiation only. The characteristics of trapping and the temperature range of hydrogen isotope retention in traps formed by prior implantation of helium depend on both the concentration of implanted helium and on the type of defects developed. The formation of helium bubbles in 18Cr10NiTi steel causes an increase in retained deuterium by one order of magnitude in the range 350-550 K in comparison with deuterium irradiation only.

Trapping by irradiation defects. Nuclear fusion reactor materials are exposed to higher densities and high temperatures of plasma with hydrogen and helium isotopes and thus large amounts of gas atoms are injected into the materials. In addition, structural materials are bombarded by high energy (14 MeV) neutrons produced in the D-T fusion reaction and radiation damage is introduced. For DT fusion neutrons with an energy of 14 MeV, a typical primary recoil atom energy for medium heavy target materials is around 400 to 1000 keV [14]. To make an appropriate choice of fusion reactor materials it is of important to gain a deep insight into the interaction between displacement damages and co-generated helium and hydrogen, because of the synergistic effect of these species arising from their mutual behavior in material.

In the present work, the concentration depth profiles of retained D atoms implanted into steel were investigated as functions of the concentration of inert gas atoms and lattice disorder resulting from argon pre-irradiation. By varying the argon implantation angle relative to the specimen we obtained different levels of damage and concentrations of argon atoms at depths between 0-100 nm. Marochov and Goodhew [15] have established that neon and argon can be used as an analogue for helium in implantation-and-annealing experiments, provided that the doses are adjusted so that the gas concentrations are equivalent. On the other hand, argon has a greater atomic mass than helium and it results in greater energy transfer during collisions, and thus, a higher dpa rate of target atoms.

Fig. 6 shows the influence of the 1.4 MeV Ar^+ pre-irradiation on retention and release of deuterium implanted in 18Cr10NiTi steel. Fig. 6,a presents the measured energy spectra of α-particles from the nuclear reaction $D(^3He,p)^4He$. Thermal release of retained D atoms from the specimen pre-irradiated with Ar ions is shown in the insert. The deuterium depth profiles deconvoluted from α-energy spectra are presented in Figs. 6, b, c. In these figures the depth distribution of the atomic displacement (dpa) and range of argon atoms calculated by the SRIM code are also plotted.

The interaction between deuterium and deuterium ion- and argon ion- induced atomic displacement damage is not strong. It is seen in Fig. 6,a that after annealing at 380 K deuterium atoms get redistributed to a greater depth, and over 500 K they localize around the argon projected range (Fig. 6,b). A high level of damage (~ 200 dpa) and C_{Ar}~1 at.% did not cause the accumulation and retention of deuterium at the depth between 0-100 nm. Fig. 6,c shows the post-annealing depth profiles of deuterium implanted at room temperature to $1\cdot10^{20}$ D/m^2 into a specimen pre-implanted with argon to $1\cdot10^{21}$ m^{-2} at an angle 30° to the surface followed by annealing at 500 K. In this case, deuterium migrates to the region of argon atom distribution, too. From this region the deuterium atoms escape when annealed at ~800 K (Fig. 6,a, insert). Argon is released at 1400 K, and the presence of deuterium does not appear to have a significant effect on the argon release spectra.

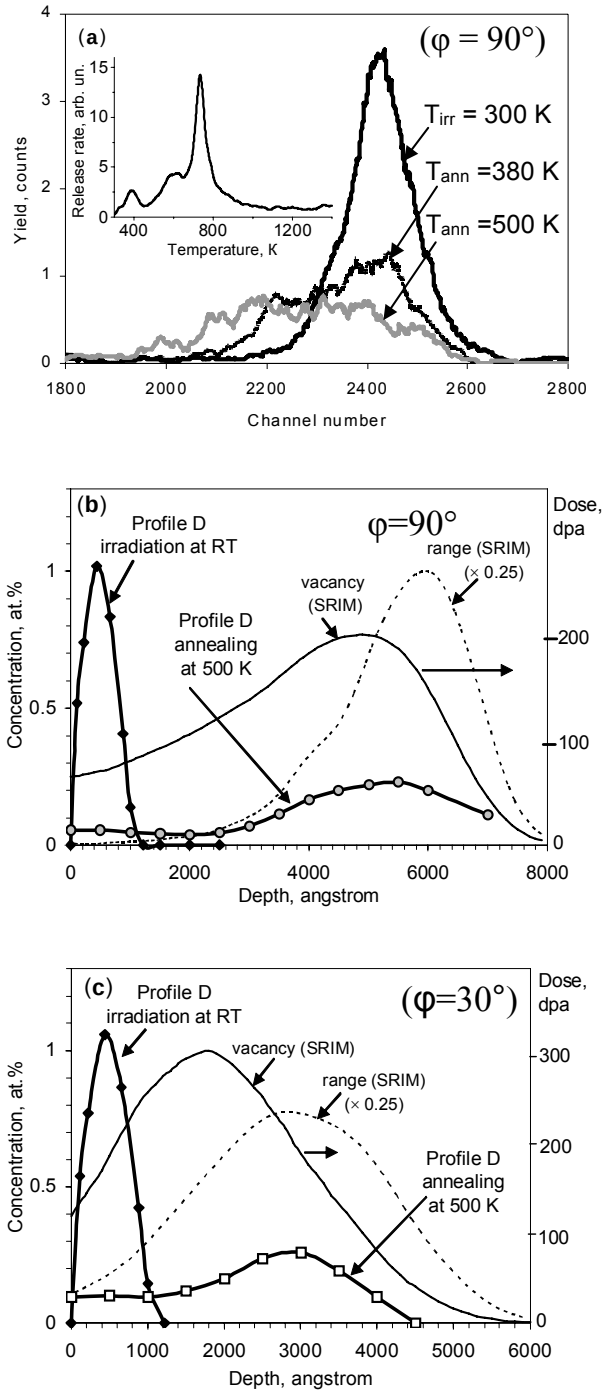

Fig. 6. Energy spectra obtained from the specimen pre-irradiated with 1.4 MeV Ar^+ and followed by implantation of 5 keV D^+ ions at RT and then annealed at temperatures between 380 and 500 K. Thermal release of retained D atoms is shown in the insert (a). The deuterium depth profiles (line with markers), the depth distribution of atomic displacements (dpa) (solid) and the range of argon atoms (dotted) calculated by the SRIM are plotted (b, c)

By processing the depth distribution profiles presented in Fig. 6 the values for deuterium retention were obtained. The temperature dependences of deuterium retention are shown in Fig. 7. The data [13] for deuterium retention in specimens pre-implanted with helium are also included.

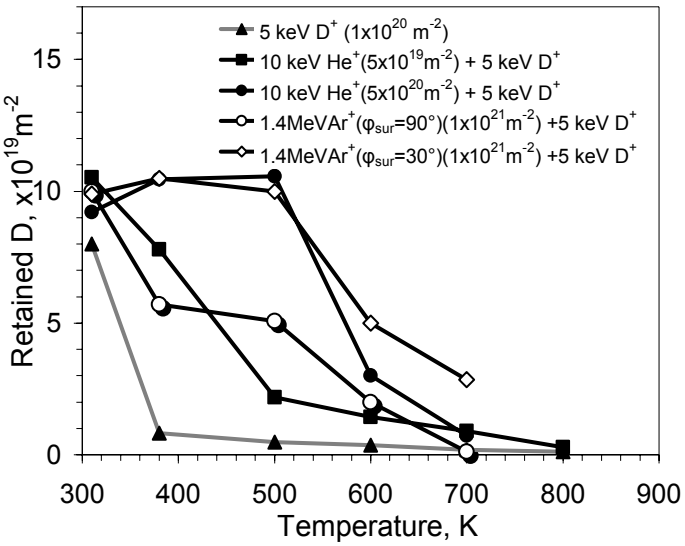

Fig. 7. Deuterium retention in 18Cr10NiTi steel implanted to $1 \cdot 10^{20}$ m^{-2} only and pre-implanted with helium to $5 \cdot 10^{19}$, $5 \cdot 10^{20}$ He/m^2, argon to $1 \cdot 10^{21}$ Ar/m^2 at angles 90 and 30° with regard to the surface

As can be seen in Fig. 7, at helium and argon pre-irradiation deuterium is retained in 18Cr10NiTi SS to annealing temperatures of ~500-600 K.

Irradiation of metals and alloys with inert gas ions generally results in the formation of microscopic gas bubbles even at RT [16]. For example, the microstructure is dominated by a high density of small cavities resulting from the precipitation of implanted helium for $0.6 \leq C_{He} \leq 3$ at.% [17]. Bubble growth and coalescence were observed when the temperature reached 573 K [17]. The investigations of crystal structure perfection, the type and number of defects examined by Rutherford backscattering spectroscopy combined with channeling have shown a flat energy dependence of the dechanneling parameter in Ni irradiated with heavy noble ions and annealed at 700 K. That indicated the bubble formation [18].

The microstructure of argon-implanted 18Cr10NiTi specimen after annealing is presented in Fig. 8. Specimens were produced as microscopic discs of 3 mm diameter. A beam of 1.4 MeV argon ions was incident at angles of 30° with regard to the surface. Specimens for electron-microscopic investigation were thinned from two sides. The layer situated at a depth of 200–300 nm from the irradiated surface was selected for analyses (see Fig. 6,c). The formation of noble-gas bubbles (mean size 4 nm, density $5.5 \cdot 10^{23}$ $м^{-3}$) is observed in the implantation layer.

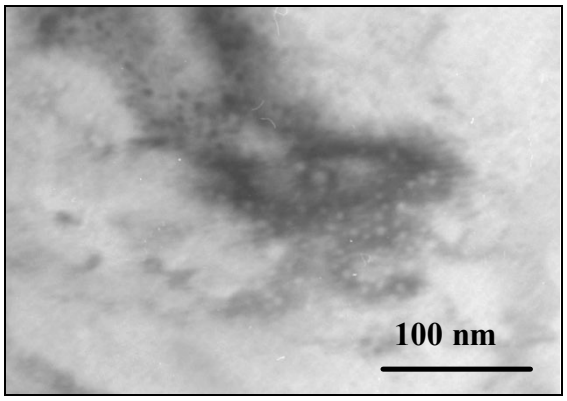

Fig. 8. Microstructure of steel 18Cr10NiTi irradiated with argon ions of 1.4 MeV energy (incident at angles of 30° with regard to the surface) at room temperature to a dose of $5 \cdot 10^{20}$ m^{-2} and annealed at 800 K

We suppose that similarly as it takes place at high-temperature implantation [19], during annealing of implanted specimens the processes of growth and coalescence of noble-gas bubbles occur, too. The detrapping of hydrogen in the temperature interval 500-600 K is probably connected with bubble system transformation. In a recent paper [20] it has been shown that helium and heavy inert gas bubbles are characterized by different strain-field contrasts.

Surface recombination rates for hydrogen in stainless steel have previously been studied by a number of researchers, using

a wide variety of methods. The investigations have demonstrated the sensitivity of surface recombination to the state of the surface oxidation.

It is known that the process of hydrogen dissociation/association at metal-vacuum interface has a significant influence on deuterium retention in metals. The back release is possible only through the formation of hydrogen molecule by way of surface recombination. The latter is governed by physical-chemical mechanisms that are highly sensitive to the surface condition and, in particular, to the surface chemical composition at the level of a fraction of a monolayer. For example, Myers [3] has indicated that electropolishing reduced the surface release rate by a factor of 1000 of that of the ion-sputtered surface. This difference is attributed to the oxide layer produced due to electrochemical treatment. Some oxidation is certainly to be expected after the exposure of samples to air.

Thermodesorption of ion-implanted deuterium from the stainless steels 06Cr18Ni10 and 12Cr18Ni10Ti that underwent different preliminary preparation has been studied. It is shown that the presence of a surface passivating film considerably shifts the gas release temperature-intervals to higher temperatures (Fig. 9).

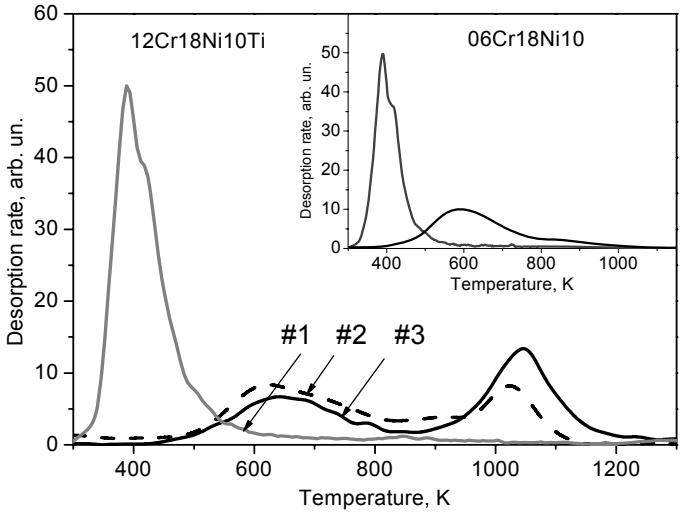

Fig. 9. The pre-treatment effects on the TDS spectra of deuterium from 12Cr18Ni10Ti and 06Cr18Ni10 steels (#1 – electro-polished and annealed; #2 – electro-polished, annealed, held in air; #3 – without electro-polishing and preliminary annealing)

Similar investigations were conducted with EI-852 steel. Ferritic/martensitic steels are one of a candidate alloys for the first wall of fusion reactors and also for the container and beam window of spallation target for accelerator driven nuclear transmutation system (ADS). The concentration depth profiles of retained D atoms implanted into EI-852 steel (its chemical composition by weight was 13.03% Cr, 2.04% Si, 1.66% Mo, 0.39% Ni, 0.33% Mn, 0.12% C, 0.008% P and 0.007% S) were investigated as functions of the concentration of inert gas atoms and lattice disorders resulting from argon pre-irradiation. The implanted particle depth distribution was measured using the nuclear reactions $D(^3He,p)^4He$ and in forward scattering geometry. By processing depth distribution profiles the values of deuterium retention were obtained. The temperature dependences of deuterium retention are shown in Fig. 10. The data [13] for deuterium retention in specimens of 18Cr10NiTi steel are also included. It has shown that the deuterium detrapping temperature range was similar to that of the austenitic stainless steels, but the amount of retained deuterium at T_{room} was less by a factor of ~3 (Fig. 10, curve 1 and 2). In the same time, for the annealing temperature higher then ~ 400 K the amount of retained in ferritic steel deuterium was by factor of ~4 more then in austenitic steel.

The damage previously created by heavy ion irradiation exert less influence on the

processes of trapping and accumulation of heavy isotopes of hydrogen–deuterium in EI-852 steel, that in austenitic steel (Fig. 10, curve 3 and 4).

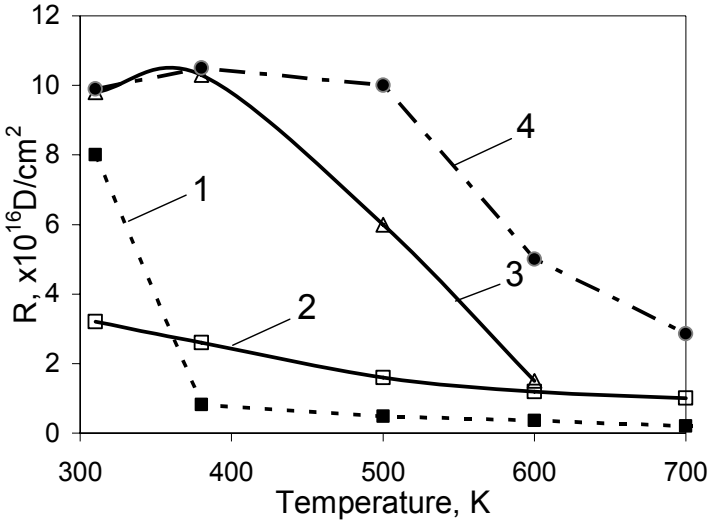

Fig. 10. Deuterium retention vs temperature over the depth of 0 to 100 nm in steels 18Cr10NiTi (1, 4) and EI-852 (2, 3) after irradiation by deuterium ions up to $1 \cdot 10^{16}$ cm^{-2} (1, 2) only and after argon pre-implantation to $5 \cdot 10^{16}$ Ar^{+}/cm^{2} (3, 4)

In the general case, the intergranular boundaries in ferritic steels promote a stronger retention of deuterium at temperatures higher than room temperature to as compared with austenitic steels, and serve as traps competitive with the radiation-created trapping sites [21].

By combining all presented results, the influence of the surface condition, preimplanted helium- and heavy ion-induced damages on deuterium trapping in austenitic and ferritic/martensitic steels can be determined. At low level of damage (~1 dpa) and clean steels surface deuterium detrapping temperature not exceed ~500 K. The efficiency of deuterium trapping is found to be less by a factor of ~3 for ferritic/martensitic steels then in austenitic steel. It is shown that the presence of surface passivating film reduced the desorption rate and considerably shifts the gas release intervals to high temperatures.

Results obtained for stainless steel 18Cr10NiTi show that pre-implantation of helium or argon causes the accumulation and retention of approximately all deuterium implanted to concentrations of 3,000 to 15,000 appm at room temperature irradiation. At preimplanted helium- or heavy ion-induced damage gas release is negligible up to temperatures of ~500 K and only above this temperature hydrogen release increases sharply (Fig. 6,a). It shows that pre-implantation of helium or argon produces new type traps for deuterium that moves the temperature intervals of its release towards the high temperature region for investigated steels. Based on the data presented above, one may assume that formation of high density bubbles (Fig. 8) resulted in strong accumulation and retention of hydrogen-deuterium isotopes in 18Cr10NiTi steel up to temperature of 800 K. This fact is confirmed by data of the 1.4 MeV Ar^{+} pre-irradiation on redistribution of deuterium implanted in 18Cr10NiTi steel (Figs. 6, 10). It is seen that after annealing at 500 K deuterium atoms get redistributed to the region of argon atom location (SRIM calculations) where the bubble formation was observed experimentally by TEM. From this region the deuterium atoms escape at annealing at about 800 K (Fig. 6).

Concluding, we provided evidence that helium and argon implantation into austenitic stainless steel 18Cr10NiTi causes the formation of traps that retain hydrogen isotopes to temperatures of around 800 K. The interaction between deuterium and deuterium ion- and argon ion-induced displacement damages is not strong as compared with inert gas bubbles. Formation of inert gas bubbles in deuterium implanted 18Cr10NiTi and EI-852 steels increases the amount of retained deuterium by one order of magnitude in the temperature range 350-600 K.

Acknowledgements

This work was performed under support of Science and Technical Center of Ukraine (Project 3663).

REFERENCES

1. F.A. Garner, B.M. Oliver, L.R. Greenwood, D.J. Edwards and S.M. Bruemer // *9th Meeting on Environmental Degradation of Materials: August 2001. Tahoe. Utah.,* p. 54–72.
2. F.A. Garner, E.P. Simonen, B.M. Oliver, L.R. Greenwood, M.L. Grossbeck, W.G. Wolfer, P.M. Scott // J. *Nucl. Mater*. 2006, v. 356, p. 122.
3. S.M. Myers, P. Nordlander, F. Besenbacher, et al. // *Phys. Rev. B*. 1986, v. 33, №2, p. 854-863.
4. S. Nagata, K. Takahiro // *J. Nucl. Mater*. 2001, v. 290-293, p. 135.
5. T. Tanaka, K. Oka. S. Ohnuki, S. Yamashita, T. Suda, S. Watanabe, E. Wakai // *J. Nucl. Mater*. 2004, v. 329-333, p. 294.
6. N. Sekimura, T. Iwai, Y. Yonamine, A.A. Naito, Y. Miwa, S. Hamada // *J. Nucl. Mater*. 2000, v. 283-287, p. 224.
7. E. Wakai, K. Kikuchi, S. Yamamoto, T. Aruga, M. Ando, H. Tanigawa, T. Taguchi, T. Sawai, K. Oka, S. Ohnuki // *J. Nucl. Mater*. 2003, v. 318, p. 267.
8. www.srim.org.
9. S.A. Karpov, I.E. Kopanets, I.M. Neklyudov, V.V. Ruzhytskiy, G.D. Tolstolutskaya // *Problems of Atomic Science and Technology (VANT). Series "Physics of Radiation Damage and Radiation Material Science".* 2003, N 83, p. 3 (in Russian).
10. V.V. Gann, G.D. Tolstolutskaya // *Nuclear Instruments and Methods in Physics Research. Section B: Beam Interactions with Materials and Atoms.* 2008, v. 266, Issue 17, p. 3365-3369.
11. J.L. Yarnell, R.H. Lonberg and W.R. Stratton // *Phys. Rev*. 1953, v. 90, p. 292.
12. S.A. Karpov, V.V. Ruzhytskiy, I.M. Neklyudov, V.I. Bendikov, G.D. Tolstolutskaya // *Metalofizika I Noveishie Teknologii.* 2004, №12, p. 1661-1670 (in Russian).
13. G.D. Tolstolutskaya, V.V. Rushytskiy, I.E. Kopanets, S.A. Karpov, V.V. Bryk, V.N. Voyevodin, F.A. Garner // *J. Nucl. Mater.* 2006, v. 356, p. 136.
14. P. Vladimirov, A. Möslang // *J. Nucl. Mater.* 2006, v. 356, p. 122.
15. N. Marochov, P.J. Goodhew // *J. Nucl. Mater.* 1988, v. 158, p. 81.
16. P. Wang, Y. Li, J. Liu, G. Zhang, R. Ma, P. Zhu, C. Qiu, T. Xu // *J. Nucl. Mater*. 1989, v. 169, p. 167.
17. A.A. Gadalla, W. Jäger, P. Ehrhart // *J. Nucl. Mater.* 1985, v. 137, p. 73.
18. G.D. Tolstolutskaya, I.E. Kopanets, I.M. Neklyudov // *Proceedings of International Conference on Charged and Neutral Particles Channeling Phenomena, Proc. SPIE*. 2007, v. 6634.
19. K. Ono, K. Arakawa, M. Oohashi, H. Kurata, K. Hojou, N. Yoshida // *J. Nucl. Mater.* 2000, v. 283-287, p. 210.
20. G. Sattonnay, L. Vincent, F. Garrido, L. Thomé // *J. Nucl. Mater*. 2006, v. 355, p. 131.
21. R. Kasada, T. Morimura, A. Hasegawa, A. Kimura // *J. Nucl. Mater.* 2001, v. 299, p. 83.

ОСОБЕННОСТИ УДЕРЖАНИЯ И ВЫХОДА ДЕЙТЕРИЯ ИЗ РАДИАЦИОННО-ИНДУЦИРОВАННЫХ ПОВРЕЖДЕНИЙ В СТАЛЯХ

Г.Д. Толстолуцкая, В.В. Ружицкий, С.А. Карпов, И.Е. Копанец

Моделирование дефектов смещения и исследование профилей распределения повреждений и примесных газовых атомов (в частности, гелия и водорода) в мишенях в широком диапазоне доз и энергий имплантируемых частиц выполнены с использованием ускорителей и ядерно-физических методов анализа. Изучено влияние предварительной имплантации гелия и создания повреждений, индуцированных имплантацией тяжелых ионов, на захват дейтерия в аустенитных и ферритно-мартенситных сталях. Результаты, полученные для стали Х18Н10Т, показывают, что ионно-имплантированный дейтерий слабо связывается дефектами, возникающими вследствие облучения стали низкоэнергетическими ионами D^+. Температурный интервал удержания газа в этом случае

составляет 300-600 К. Характеристики захвата и температурные интервалы удержания водорода ловушками, образованными при предварительной имплантации гелия, зависят от концентрации внедренного гелия и типа возникающих ловушек. Образование гелиевых пузырьков в стали Х18Н10Т приводит к увеличению на порядок количества дейтерия, удерживаемого в интервале температур 300-600 К, а также к расширению интервала его эффективного захвата до 1000 К. Облучение высокоэнергетичными тяжелыми ионами (1.4 МэВ Ar^+) использовали для моделирования образующихся в каскадах столкновений кластеров дефектов, характерных для термоядерных реакторов. В этом случае было обнаружено значительное увеличение удержания водорода и дейтерия. Показано, что присутствие поверхностной пассивационной пленки значительно смещает интервал выхода газа в сторону высоких температур и уменьшает коэффициент поверхностной рекомбинации дейтерия на несколько порядков величины.

ОСОБЛИВОСТІ УТРИМАННЯ І ВИХОДУ ДЕЙТЕРІЮ З РАДІАЦІЙНО-ІНДУКОВАНИХ ПОШКОДЖЕНЬ В СТАЛЯХ

Г.Д. Толстолуцька, В.В. Ружицький, С.О. Карпов, І.Є. Копанець

Моделювання дефектів зміщення і дослідження профілів розподілу пошкоджень і домішкових газових атомів (зокрема, гелію та водню) у мішенях в широкому діапазоні доз і енергій частинок, що імплантуються, виконані з використанням прискорювачів і ядерно-фізичних методів аналізу. Вивчений вплив попередньої імплантації гелію і створення пошкоджень, індукованих імплантацією важких іонів, на захоплення дейтерію в аустенітних і феритно-мартенситних сталях. Результати, отримані для сталі Х18Н10Т, показують, що іонно-імплантований дейтерій слабо зв'язується дефектами, які виникають внаслідок опромінення сталі низькоенергетичними іонами D^+. Температурний інтервал утримання газу в цьому випадку становить 300-600 К. Характеристики захоплення і температурні інтервали утримання водню пастками, утвореними при попередній імплантації гелію, залежать від концентрації проникого гелію і типу пасток, що виникають. Утворення гелієвих бульбашок в сталі Х18Н10Т призводить до збільшення на порядок кількості дейтерію, що утримується в інтервалі температур 300-600 К, а також до розширення інтервалу його ефективного захоплення до 1000 К. Опромінювання високоенергетичними важкими іонами (1.4 МеВ Ar^+) використовували для моделювання кластерів дефектів, які утворюються в каскадах зіткнень і є характерними для термоядерних реакторів. В цьому випадку було виявлено значне збільшення утримання водню і дейтерію. Показано, що присутність поверхневої пасивуючої плівки значно переміщує інтервал виходу газу у бік високих температур і зменшує коефіцієнт поверхневої рекомбінації дейтерію на декілька порядків величини.